Translational Oncology 13 (2020) 100742

Contents lists available at ScienceDirect

Translational Oncology

journal homepage: www.elsevier.com/locate/tranon

Lipiodol as an Imaging Biomarker of Tumor Response After Conventional Transarterial Chemoembolization: Prospective Clinical Validation in Patients with Primary and Secondary Liver Cancer

Milena A. Miszczuk [a,b,1], Julius Chapiro [a,1], Jean-Francois H. Geschwind [d], Vinayak Thakur [a], Nariman Nezami [a], Fabian Laage-Gaupp [a], Michal Kulon [a], Johanna M.M. van Breugel [a,e], Arash Fereydooni [a], MingDe Lin [a,c], Lynn Jeanette Savic [a,b], Bruno Tegel [a,b], Tamara Wahlin [f], Eliot Funai [a], Todd Schlachter [a,*]

[a] Department of Radiology and Biomedical Imaging, Yale School of Medicine, 333 Cedar Street, New Haven, CT, 06520, USA
[b] Institute of Radiology, Charité-Universitätsmedizin Berlin, corporate member of Freie Universität Berlin, Humboldt-Universität, and Berlin Institute of Health, 10117 Berlin, Germany
[c] Visage Imaging, Inc., 12625 High Bluff Drive, Suite 205, San Diego, CA 92130, USA
[d] PreScience Labs/Cage Pharma, 1812 Ashland Avenue, Baltimore, MD 21205, USA
[e] University Medical Center Utrecht, Imaging department, Utrecht, The Netherlands
[f] University of California, San Diego, 9500 Gilman Dr, La Jolla, CA 92093

ARTICLE INFO

Article history:
Received 18 August 2019
Received in revised form 9 January 2020
Accepted 13 January 2020
Available online xxxx

ABSTRACT

PURPOSE: To prospectively investigate whether Lipiodol can be used as a potential imaging biomarker of tumor response after conventional transarterial chemoembolization (cTACE) for both primary and secondary liver cancer. ***MATERIALS AND METHODS:*** This prospective single-center single-arm clinical trial enrolled a total of 39 patients with primary or secondary liver malignancy [hepatocellular carcinoma (HCC), $n = 22$ and non-HCC, $n = 17$]. Patients were treated with cTACE according to a standardized protocol and underwent multimodality imaging at baseline [magnetic resonance imaging (MRI)/computed tomography (CT)/positron emission tomography (PET)]; at 24 hours post-TACE (CT); and at 30, 90, and 180 days post-TACE (MRI/CT/PET). Image data analysis included quantitative assessment of tumor characteristics, Lipiodol deposition, fluorodeoxyglucose uptake, and tumor response assessment. Statistical analysis included linear regression, Student's *t* tests, Wilcoxon rank sum and signed rank test, Chi-square, and Fisher's exact test. ***RESULTS:*** Image analysis demonstrated that baseline tumor diameter ($R^2 = 0.4$, $P = .0001$), area ($R^2 = 0.45$, $P < .0001$), volume ($R^2 = 0.3$, $P < .002$), and enhancing volume (cm^3, $R^2 = 0.23$, $P < .002$) at baseline correlated inversely with Lipiodol tumor coverage and response rates. Baseline tumor enhancement in % of the total tumor was the only parameter to positively correlate with Lipiodol coverage ($R^2 = 0.189$, $P = .0456$). Patients with high Lipiodol coverage of the tumors showed a higher tumor quantitative European Association for the Study of the Liver response rate at 30-day follow-up ($P = .004$). Lipiodol retention in both primary and secondary liver tumors was sustained over time, while nontarget hepatic deposits demonstrated near-complete elimination at 30-day follow-up ($P < .001$). ***CONCLUSION:*** Lipiodol deposition in liver tumors can be predicted using quantitative baseline imaging characteristics and correlates with tumor response. This supports another role for Lipiodol, namely, that of an imaging biomarker of tumor response after cTACE.

Introduction

The management of primary and metastatic liver cancer constitutes a significant oncologic challenge. Despite recent progress in the treatment of hepatocellular carcinoma (HCC), it remains plagued by a growing incidence and a consistently high mortality rate as it is the fourth most common cause of cancer-related deaths worldwide [1]. Curative treatments for HCC are only applicable to a minority of patients as nearly 70% are diagnosed at more advanced stages of the disease. For such patients, palliative transarterial catheter-based therapies and systemic therapy are the only available options [2–4].

Over the last three decades, image-guided intra-arterial therapies (IATs) have been validated through well-designed clinical trials and incorporated into treatment guidelines as a result [5,6]. Among the various IATs, conventional transarterial chemoembolization (cTACE) using ethiodized oil (Lipiodol, Guerbet) combined with chemotherapeutic agents has been the most frequently used and studied option to the point that level 1A evidence

* Address all correspondence to: Todd Schlachter, Department of Radiology and Biomedical Imaging, Yale School of Medicine, 333 Cedar Street, New Haven, CT, 06520, USA.
E-mail address: todd.schlachter@yale.edu. (T. Schlachter).
[1] Both authors contributed equally to this work.

http://dx.doi.org/10.1016/j.tranon.2020.01.003

exists, demonstrating its impact on patient survival and establishing cTACE as the recommended therapy for patients with intermediate-stage HCC in guidelines [3,7–10]. The data are less robust for patients with liver metastases who have progressed through systemic drug therapy; cTACE has nonetheless been shown through small studies to improve patient survival in the salvage setting [11–14].

Lipiodol plays a unique multifunctional role in cTACE. Beyond its well-established function as a drug carrier, it is also used as an imaging agent during cTACE as well as on intraprocedural cone-beam computed tomography (CB-CT) and postprocedural multidetector CT [15]. Another potential role of Lipiodol is that of a marker of tumor response. It has been demonstrated at histopathology that Lipiodol retention within tumors can be reliably used as direct evidence of tumor necrosis [16,17]. Furthermore, specific baseline imaging features, especially tumor vascularity, may be useful to predetermine Lipiodol deposition and thus predict therapeutic efficacy [18,19]. As a result, such imaging features at baseline could be used to select the best tumors for cTACE.

This prospective clinical study was designed to investigate whether Lipiodol can be used reliably as an imaging biomarker of tumor response after cTACE across a spectrum of tumor types that included both primary and secondary liver cancer. A multimodality imaging protocol including CT, magnetic resonance imaging (MRI), and positron emission tomography (PET) was used for that purpose.

Materials and Methods

Study Cohort

This prospective single-center single-arm clinical trial enrolled patients with primary or secondary liver malignancy. It was conducted in accordance with the Declaration of Helsinki on Ethical Principles for Medical Research Involving Human Subjects, approval from the Institutional Review Board was obtained, and the study was registered at clinicaltrials.gov (NCT01877187). Eligible patients were identified and recruited by a multidisciplinary team. A total of 39 patients (HCC, $n = 22$ and non-HCC, $n = 17$) were included in this trial and treated with cTACE between 2013 and 2015. For detailed inclusion and exclusion criteria, see Supplementary material.

Study Design

After obtaining written informed consent, patients underwent baseline assessment within 30 days prior to cTACE (see Figure 1). Baseline preprocedural imaging included multiphasic contrast-enhanced (CE) CT, multiphasic CE-MRI scan of the liver, and fluorodeoxyglucose (FDG)-PET/CT scans. Patients underwent treatment with cTACE followed by a noncontrast CT scan of the abdomen 24 hours after the procedure. Follow-up imaging and clinical evaluation were done at 30, 90, and 180 days after TACE. This included physical examination, laboratory tests, tumor marker analysis, multiphase CE-CT and CE-MRI of the liver, and PET-CT scan (only 90 and 180 days of follow-up). Adverse events (AEs) were documented. Patients underwent cTACE procedure as described in previous studies [20] and in the Supplementary material.

Imaging Data Analysis

Linear measurements were done using standardized electronic calipers on slices with the largest tumor diameter. Target tumors were defined as dominant liver tumors treated during the first cTACE. A maximum of two target tumors per patient were chosen for tumor response analysis. Measurements of the longest tumor diameter (cm) and area (cm^2) as well as the longest enhancing tumor diameter (cm) and enhancing area (cm^2) were performed.

The same tumors were segmented on pre- and posttreatment CE-MRI scans (using a semiautomatic, threshold-based 3D segmentation technique, IntelliSpace Portal V 8.0, Philips). Using image subtraction and placement of a region of interest, tumor volume [TV (cm^3)] and enhancing tumor volume [ETV (cm^3)] calculations were performed. Enhancing tumor volume was defined using previously validated quantitative European Association for the Study of the Liver (qEASL) methodology [21].

Target tumor Lipiodol deposition and washout were quantified using the previously described 3D tumor segmentation and quantification approach on the noncontrast follow-up CT scans (24 hours and 30, 90, and 180 days). Nontumorous liver parenchymal Lipiodol deposition and washout were assessed by quantifying the nontarget Lipiodol deposits after embolization using the aforementioned 3D quantitative technique (see Supplementary material).

Tumor response assessment was done using World Health Organization (WHO), Response Evaluation Criteria in Solid Tumors (RECIST), modified RECIST (mRECIST), European Association for the Study of the Liver (EASL), and quantitative EASL (qEASL) guidelines [21–26]. Tumor response was categorized into complete response (CR), partial response (PR), stable disease (SD), and progressive disease (PD). Patients with CR and PR were considered as responders (R), while patients with SD and PD were considered as nonresponders (NR).

Tumor burden (TB), enhancing tumor burden [ETB, (%)], and liver volume measurements were performed as described in previous studies [27] and in the Supplementary material.

PET-CT scans were being evaluated for their ability to predict and reliably assess tumor response in the setting of liver directed locoregional therapy. The radioactive dose of FDG dose is based on patient weight, 0.09 mCi/lb (minimum 10 mCi, maximum 25 mCi). The FDG was sourced from PETNET Solutions Inc., a subsidiary of Siemens Medical Solutions USA, Inc. The mean and maximum standardized uptake values (SUVs) of the target tumors, liver, and blood pools pre- and posttreatment were measured. All measurements were performed using MIM 6.6.6 (MIM Software).

Study Endpoints

Tumor response was the primary endpoint of the study. Several secondary imaging endpoints were analyzed in subgroups to assess the following correlations:

1. Correlation between baseline tumor characteristics (tumor enhancement, TV, ETV, TB, ETB) and Lipiodol deposition at 24-hour noncontrast CT
2. Correlation between baseline tumor characteristics and response
3. Correlation between baseline tumor characteristics and SUV on baseline imaging
4. Correlation between Lipiodol deposition in 24-hour noncontrast CT and SUV on baseline and follow-up imaging
5. Correlation between SUV on baseline and follow-up imaging and response
6. Correlation between Lipiodol deposition in 24-hour noncontrast CT and response
7. Intra- versus extratumoral Lipiodol washout

Correlation analysis was done for the whole group, as well as for subgroups as stratified by tumor type (HCC vs. non-HCC). The multi–time point analysis included patients who underwent a single session of cTACE. Imaging acquired after retreatment ($n = 7$) was excluded from this post hoc analysis. Additional characterizations and inclusion and exclusion criteria for each analyzed subgroup (1-7) are specified in Table 1. Overall survival and the occurrence of adverse events were analyzed as additional secondary endpoints.

Statistical Analysis

To summarize the data in absolute numbers and percentages, descriptive statistics were used. For continuous variables, mean and range were

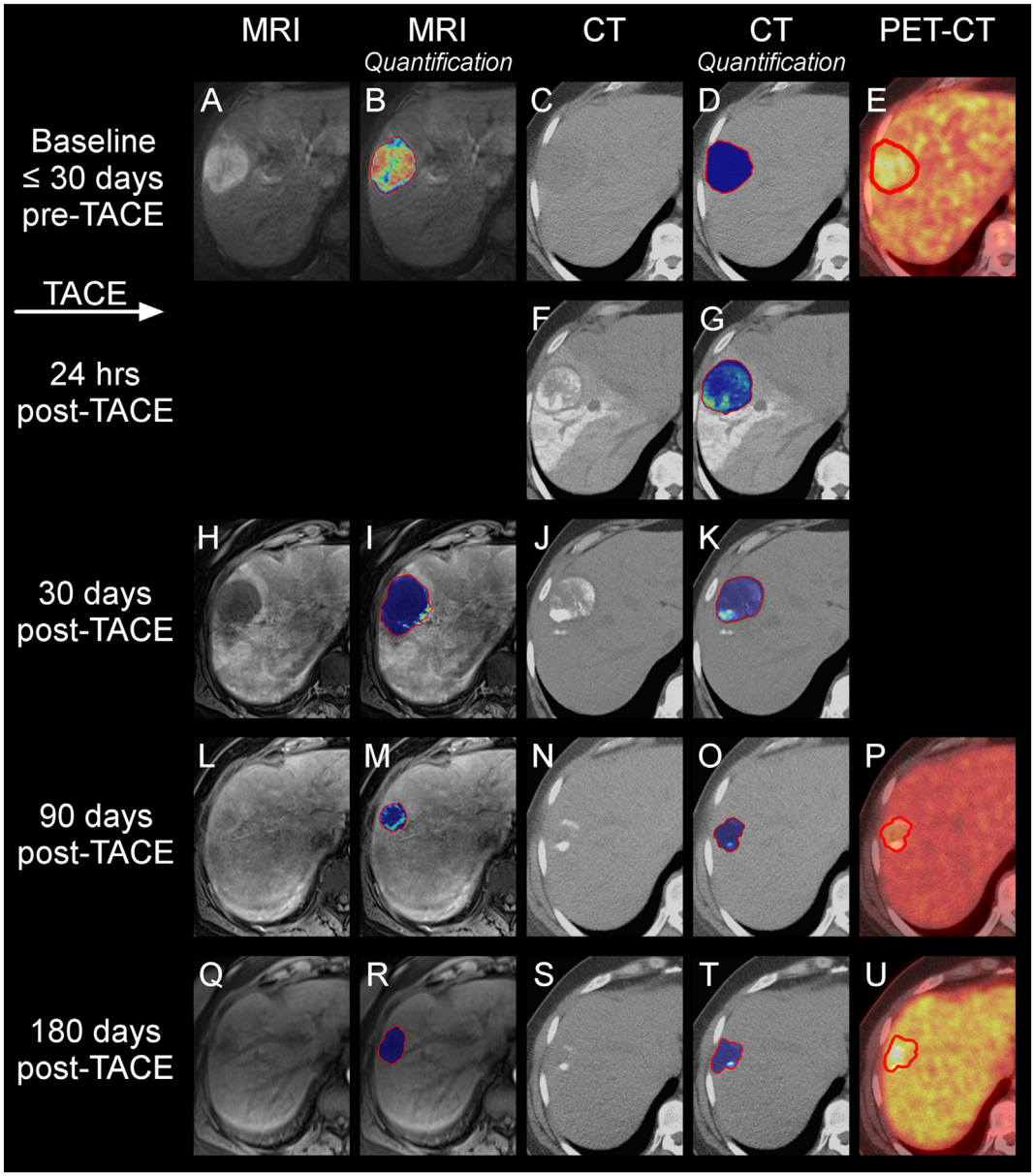

Figure 1. Overview presenting the collected imaging data. (A) Baseline contrast-enhanced (CE) MRI, (B) baseline CE-MRI + qEASL, (C) baseline native CT, (D) baseline native CT + qEASL, (E) baseline PET-CT, (F) 24-hour follow-up: native CT, (G) 24-hour follow-up: native CT + qEASL, (H) 30-day follow-up: CE-MRI, (I) 30-day follow-up: CE-MRI + qEASL, (J) 30-day follow-up: native CT, (K) 30-day follow-up: native CT + qEASL, (L) 90-day follow-up: CE-MRI, (M) 90-day follow-up: CE-MRI + qEASL, (N) 90-day follow-up: native CT, (O) 90-day follow-up: native CT + qEASL, (P) 90-day follow-up: PET-CT, (Q) 180-day follow-up: CE-MRI, (R) 180-day follow-up: CE-MRI + qEASL, (S) 180-day follow-up: native CT, (T) 180-day follow-up: native CT + qEASL, (U) 180-day follow-up: PET-CT.

calculated. To establish the correlation between values, linear regression model, Student's *t* tests, Wilcoxon rank sum test, Wilcoxon signed rank test, Chi-square tests, and Fisher's exact test were used. Survival analysis included calculation of the median overall survival (MOS), defined as time from the first TACE to the date of death. Patients receiving retreatment or lost in follow-up were censored. Statistical significance was defined as $P \leq .05$. The analysis was performed using the statistical software SAS (SAS Institute, Version 9.4.3).

Results

Study Cohort and Treatment

A total of 39 patients with primary or secondary liver cancer were enrolled into this study (Table 2). Twenty-two patients had HCC; 17 patients had metastatic liver cancer, including neuroendocrine tumors ($n = 7$), cholangiocarcinoma ($n = 8$), cutaneous melanoma ($n = 1$), and uveal melanoma ($n = 1$). Detailed description of the study cohort is provided in the Supplementary material. MOS of the entire cohort was 18.02 months.

Correlation Between Baseline Tumor Characteristics and Lipiodol Deposition at the Initial (24-Hour) Follow-up

All measures of tumor size (tumor diameter, area, or volume) demonstrated a statistically significant, inverse correlation with Lipiodol deposition of the targeted tumors, with higher statistical significance for the patients with metastatic liver cancer (Table 4), indicating that larger tumor size at baseline is a negative predictor of high Lipiodol deposition, especially in metastatic liver tumors. As for the enhancement-based tumor characteristics, a reverse trend was observed for baseline tumor enhancement expressed in percentage of total tumor volume, indicating that hyperenhancing tumors were more likely to deposit more Lipiodol after cTACE ($R^2 = 0.189$, $P = .0456$).

Table 1
An Overview Presenting the Inclusion and Exclusion Process of Suitable Patient Groups for Each Research Question

Research Question	*N*	Patient Inclusion and Exclusion Criteria
Baseline tumor characteristics and Lipiodol deposition	$N = 37$	*Inclusion criteria:* ●CE-MRI on baseline *Exclusion criteria:* ●Corrupted MRI imaging data on baseline ($n = 2$)
Baseline tumor characteristics and response	$N = 30$	*Inclusion criteria:* ●CE-MRI on baseline ●At least 30-day follow-up *Exclusion criteria:* ●Missing CE phases on 30-day follow-up due to existing contraindications ($n = 2$) ●Corrupted MRI imaging data on baseline ($n = 2$) ●Missing follow-up ($n = 5$)
Baseline tumor characteristics and SUV on baseline	$N = 35$	*Inclusion criteria:* ●CE-MRI on baseline ●PET-CT on baseline *Exclusion criteria:* ●Missing PET-CT on baseline ($n = 2$) ●Corrupted MRI imaging data on baseline ($n = 2$)
Lipiodol deposition in 24-h CT and SUV on baseline and follow-up	$N = 37$	*Inclusion criteria:* ●PET-CT on baseline ●Initial CT follow-up *Exclusion criteria:* ●Missing PET-CT on baseline ($n = 2$)
SUV on baseline and follow-up and response	$N = 30$	*Inclusion criteria:* ●CE-MRI on baseline ●PET-CT on baseline ●At least 30-day follow-up *Exclusion criteria:* ●Missing PET-CT on baseline ($n = 2$) ●Corrupted MRI imaging data on baseline ($n = 2$) ●Missing contrast-enhanced phases on 30-day follow-up due to existing contraindications ($n = 2$) ●Missing follow-up ($n = 3$)
Lipiodol deposition in 24-h CT and response	$N = 30$	*Inclusion criteria:* ●CE-MRI on baseline ●At least 30-day follow-up *Exclusion criteria:* ●Missing CE phases on 30-day follow-up due to existing contraindications ($n = 2$) ●Corrupted MRI imaging data on baseline ($n = 2$) ●Missing follow-up ($n = 5$)
Intra- and extratumoral Lipiodol washout	$N = 23$	*Inclusion criteria:* ●At least 30-day native CT follow-up *Exclusion criteria:* ●Missing CT follow-up ($n = 10$) ●Missing native CT phases on follow-up ($n = 6$)

Correlation Between Baseline Tumor Characteristics and Tumor Response

Response rates are provided in Table 3. Responders (EASL, 30-day time point) were overall more likely to have a smaller median tumor diameter ($P = .025$) and median tumor area ($P = .043$) at baseline imaging as compared with nonresponders. They were also more likely to demonstrate arterially hyperenhancing tumors at baseline imaging than nonresponders ($P = .020$). A similar trend was demonstrated at the 90-day imaging time point across all response criteria with the exception of RECIST, showing consistently greater response rates for arterially hyperenhancing tumors at baseline (WHO $P = .017$, mRECIST $P = .011$, EASL $P = .029$, and qEASL $P = .013$). For RECIST, this trend was only confirmed for patients who demonstrated a response at the 180-day imaging follow-up ($P = .034$). Both anatomical and enhancement-based measurements decreased over time, indicating a tumor shrinkage and decrease of tumor enhancement (Figure 2). As for the FDG uptake, we observed a decrease of mean SUV as well as tumor/liver and tumor/blood ratios.

Correlation Between Baseline Tumor Characteristics and FDG Uptake

HCC tumors with a larger tumor size at baseline were more likely to demonstrate increased FDG uptake (as measured in SUV) at baseline PET-CT with highly significant *P* values ($P > .01$) and strong positive correlation ($R^2 > 0.5$; Table 5). Baseline arterial enhancement showed a similar but weaker trend with significance only achieved for unidimensional measurements. No significant correlation was noted between baseline tumor characteristics and FDG uptake in the metastatic liver cancer group ($P > .05$).

Correlation Between Lipiodol Deposition on 24-Hour CT and FDG Uptake at Baseline and Follow-up Imaging

There was no statistically significant correlation between Lipiodol deposition and tumor coverage as seen on the CT 24 hours after cTACE and FDG uptake at baseline or any follow-up time point for the overall cohort, as well as for the HCC and metastatic liver cancer subgroups ($P > .05$).

Correlation Between FDG Uptake at Baseline and Follow-up Imaging and Response on Follow-up Imaging

mRECIST responders (total cohort, 30-day time point) had significantly lower mean SUV ($P = .015$), tumor/liver ratio ($P = .013$), and tumor/blood ratio ($P = .013$) at baseline PET-CT. EASL and qEASL responders (total cohort, 30-day time point), had significantly lower mean SUV on baseline PET-CT ($P = .031$ and $P = .037$ for

Table 2
Baseline Characteristics of the Cohort

Parameter	All Patients (Mean)	HCC (Mean)	Non-HCC (Mean)
Demographics:			
Age (years)	61.28 (10.75)	61.68 (8.83)	60.76 (13.10)
Gender (male/female)	26/13	18/4	8/9
Ethnicity			
White	23	10	13
African American	10	10	0
Hispanic	1	0	1
Other	5	2	3
Tumor type			
HCC	22	22	N/A
Neuroendocrine: GI	4	N/A	4
Neuroendocrine: pancreatic	2	N/A	2
Neuroendocrine: bronchial	1	N/A	1
Cholangiocarcinoma	8	N/A	8
Cutaneous melanoma	1	N/A	1
Uveal melanoma	1	N/A	1
Clinical history and treatment			
HBV	2	2	0
HCV	17	17	0
Cirrhosis	20	20	0
TACE prior to enrollment	6	5	1
Child-Pugh score (A/B/C)	29/9/1	13/8/1	16/1/0
ECOG performance status (0/1/2)	22/15/2	14/7/1	8/8/1
BCLC (A/B/C/D)		7/6/8/1	N/A
Treatment with sorafenib	4	4	N/A
Baseline imaging characteristics			
Tumor diameter (cm)	7.47 (4.36)	5.14 (3.09)	10.49 (3.92)
Enhancing tumor diameter (cm)	5.36 (2.82)	4.04 (2.34)	24.35 (21.89)
Tumor area (cm^2)	35.97 (41.19)	19.01 (23.63)	57.93 (48.88)
Enhancing tumor area (cm^2)	15.68 (17.37)	8.98 (8.54)	24.35 (21.89)
Tumor volume (cm^3)	233.06 (451.40)	82.55 (120.29)	410.13 (616.15)
Enhancing tumor volume (cm^3)	130.84 (299.64)	40.93 (73.11)	236.63 (416.74)
Tumor enhancement (%)	55.50 (29.16)	56.02 (32.03)	54.88 (26.34)
Tumor burden (%)	10.12 (13.44)	4.93 (6.62)	16.23 (16.77)
Enhancing tumor burden (%)	5.70 (9.24)	2.64 (4.25)	9.30 (12.04)
Liver volume (cm^3)	1823.57 (789.66)	1561.41 (558.78)	2131.99 (919.38)
SUV mean	4.95 (4.35)	3.58 (1.66)	6.57 (5.85)
SUV: lesion/liver ratio	2.32 (2.09)	1.69 (0.85)	3.05 (2.81)
SUV: lesion/blood ratio	3.08 (3.04)	2.09 (1.03)	4.23 (4.11)

BCLC, Barcelona Clinic Liver Cancer staging; ECOG, Eastern Cooperative Oncology Group; HBV, hepatitis B virus; HCV, hepatitis C virus.

EASL and qEASL, respectively). No correlation between FDG uptake at baseline and tumor response on 90- and 180-day follow-up imaging was seen for any response criteria ($P > .05$). Importantly, no correlation between FDG uptake on postprocedural PET-CTs and MRI-based tumor response on follow-up scans was seen for any assessment method and subgroup ($P > .05$).

Correlation Between Lipiodol Deposition on the 24-Hour CT and Response on Follow-up MRI

Lipiodol deposition was greater in qEASL responders (30-day time point; measured in % of the tumor volume covered) than in the non-responders, as quantified on the 24-hour CT follow-up scans. This

Table 3
Response Rates of the Cohort

	30 days			
	HCC		*Non-HCC*	
	R	NR	R	NR
WHO	2 (11.1%)	16 (88.9%)	1 (6.3%)	15 (93.8%)
RECIST	1 (5.6%)	17 (94.4%)	1 (6.3%)	15 (93.8%)
mRECIST	9 (50%)	9 (50%)	2 (14.3%)	12 (85.7%)
EASL	11 (61.1%)	7 (28.9%)	2 (14.3%)	12 (85.7%)
qEASL	6 (37.5%)	10 (62.5%)	1 (7.1%)	13 (92.9%)
		90 days		
WHO	4 (36.4%)	7 (63.6%)	3 (42.9%)	4 (57.1%)
RECIST	5 (45.5%)	6 (54.5%)	3 (42.9%)	4 (57.1%)
mRECIST	6 (54.5%)	5 (45.5%)	3 (42.9%)	4 (57.1%)
EASL	7 (63.6%)	4 (36.4%)	5 (71.4%)	2 (28.6%)
qEASL	5 (55.6%)	4 (44.4%)	4 (57.1%)	3 (42.9%)
		180 days		
WHO	4 (36.4%)	7 (63.6%)	2 (40%)	3 (60%)
RECIST	4 (36.4%)	7 (63.6%)	2 (40%)	3 (60%)
mRECIST	6 (54.5%)	5 (45.5%)	2 (40%)	3 (60%)
EASL	7 (63.6%)	4 (36.4%)	4 (80%)	1 (20%)
qEASL	6 (66.7%)	3 (33.3%)	5 (100%)	0 (0%)

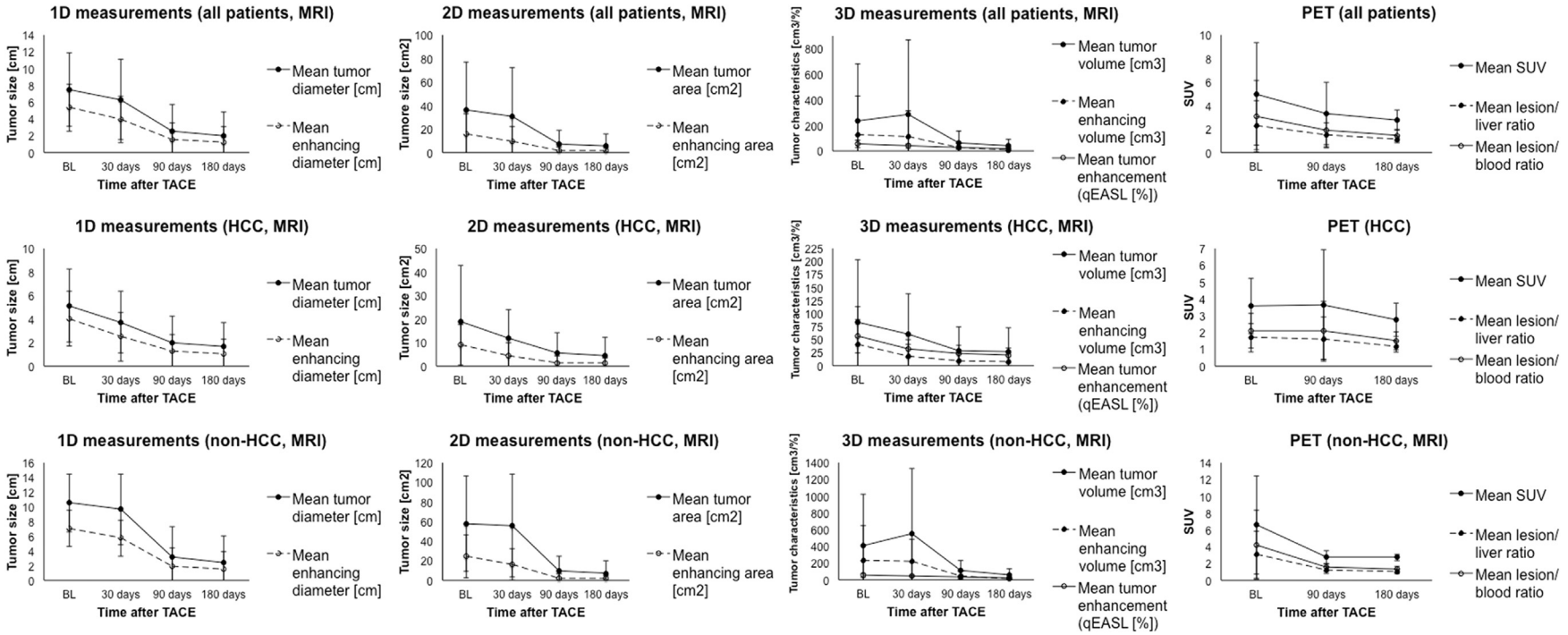

Figure 2. Tumor characteristics over time, presented for the entire cohort, as well as stratified by tumor type (HCC and metastatic).

Table 4
An Overview Presenting the Association of the Baseline Tumor Characteristics and Lipiodol Deposition on the Initial CT Follow-up

	All Patients		HCC		Non-HCC	
	R^2	*P* Value	R^2	*P* Value	R^2	*P* Value
Tumor diameter (cm)	0.407	.0001	0.242	.0201	0.428	.0044
Enhancing tumor diameter (cm)	0.216	.0337	-	>.05	-	>.05
Tumor area (cm^2)	0.452	<.0001	0.209	.0322	0.550	.0007
Enhancing tumor area (cm^2)	0.297	.0037	-	>.05	0.302	.0224
Tumor volume (cm^3)	0.311	.0021	-	>.05	0.368	.0098
Enhancing tumor volume (cm^3)	0.227	.0181	-	>.05	0.255	.0386
Tumor enhancement (% lesion)	*0.189	*.0456	-	>.05	-	>.05
Tumor burden (% liver)	0.320	.0017	-	>.05	0.393	.0071
Enhancing tumor burden (% liver)	0.200	.0348	-	>.05	-	>.05

The asterisked R^2 and *P* values were the only ones to demonstrate a statistically significant and positive correlation between parameters.

difference was significant both for the entire cohort ($P = .004$) and the HCC patients ($P = .026$) but not for the non-HCC subgroup ($P > .05$).

Lipiodol Washout Over Time in Tumor and Liver Tissue

Target tumor coverage with Lipiodol (expressed as % of the tumor volume covered on the 24-hour post-cTACE CT scan) initially did not significantly differ between HCC and metastatic liver tumors ($P = .08$), with HCC tumors showing a trend towards better coverage (Figure 3). When measured at the 30- and 90-day imaging time points after cTACE, the rate of Lipiodol retention and sustained coverage was greater in HCC tumors than in metastatic liver tumors ($P = .03$ and $P = .008$ for the 30- and 90-day follow-up, respectively). Lipiodol was eliminated from the background liver parenchyma as soon as 30 days after cTACE, with washout rates that were significantly higher than those in tumors of the entire cohort and of the HCC subgroup ($P < .001$ and $P < .001$, respectively). Lipiodol elimination from nontumorous liver parenchyma with underlying cirrhosis (in patients with HCC) was not significantly different from that observed in noncirrhotic livers ($P > .3$, cirrhosis rate in HCC cohort = 100%, non-HCC = 0%).

Discussion

The results of this prospective clinical trial describe the dynamic role of Lipiodol as an imaging biomarker following cTACE across a spectrum of tumor types and sizes within the liver. The strength of our study lies in its design to monitor the patterns of Lipiodol deposition and longitudinal retention within liver tumors. The data support that Lipiodol deposition in targeted tumors can be predicted before the procedure using quantitative assessment of baseline tumor enhancement and that the correlation between Lipiodol deposition within the tumor and tumor response was strong and statistically significant.

Our study elucidated clinically relevant imaging findings when performing cTACE: first, arterially hyperenhancing tumors at baseline imaging are more likely to respond to cTACE; second, small HCC nodules showed higher Lipiodol deposition than larger HCCs; third, the greater Lipiodol deposition in small HCC nodules resulted in better clinical outcomes in terms of patient survival, confirming what had been reported in other studies [19,28,30,33]; and fourth, the extent of Lipiodol deposition within tumors as assessed by both intra- and postprocedure CT is able to predict tumor response using enhancement-based criteria. As a result, it is clear that Lipiodol is able to fulfill its many roles as a contrast, drug delivery, and microembolic agent and as a biomarker of tumor response [38].

The concept of theranostic agents was introduced in the mid-1980s for agents characterized by multifaceted capabilities [39], mainly able to serve the purpose of diagnosis, drug delivery, and disease monitoring [40]. Lipiodol, when emulsified and administered selectively into the liver, possesses such key characteristics. Our data support that Lipiodol can be used as an imaging biomarker of tumor response because of its unique ability to predict outcomes after cTACE. The data confirmed our hypothesis that Lipiodol deposition is indeed taken up by tumors relatively specifically and more importantly remains in tumors for a long period of time. Lipiodol deposition was tumor-dominant with a seemingly greater affinity for HCC and more importantly remains in tumors for a long period of time. This was the case mostly in HCC where Lipiodol was retained at all imaging follow-up time points, whereas it was not as evident in metastatic liver tumors. Conversely, near-complete elimination of Lipiodol from nontumorous liver parenchyma was observed in both cirrhotic and noncirrhotic livers.

The role of Lipiodol as a potential biomarker of tumor necrosis, and therefore response, has been reported on for nearly two decades, with most of the data coming from retrospective studies. Lipiodol deposition was reported to be greatest in small tumors and associated with better outcomes and longer survival [17,23–25]. Additionally, Lipiodol was also found to accumulate preferentially in arterially hyperenhancing tumors [26]. Our data prospectively validate both hypotheses: (1) by confirming the inverse correlation between tumor size and Lipiodol deposition and (2) by demonstrating that Lipiodol preferentially accumulates in hyperenhancing tumors.

Table 5
An Overview Presenting the Association of the Baseline Tumor Characteristics and the FDG Uptake, Results for the HCC Patients

	Mean SUV		Lesion/Liver Ratio		Lesion/Blood Ratio	
	R^2	*P* Value	R^2	*P* Value	R^2	*P* Value
Tumor diameter	0.617	.0001	0.724	<.0001	0.737	<.0001
Enhancing diameter	0.409	.0043	0.571	.0003	0.530	.0006
Tumor area	0.622	.0001	0.678	<.0001	0.706	<.0001
Enhancing area	-	>.05	0.272	.0265	-	>.05
Tumor volume	0.526	.0007	0.654	<.0001	0.698	<.0001
Enhancing tumor volume	-	>.05	-	>.05	0.253	.0253
Tumor enhancement	-	>.05	-	>.05	-	>.05
Tumor burden	0.503	.0010	0.575	.0003	0.663	<.0001
Enhancing tumor burden	-	>.05	-	>.05	-	>.05

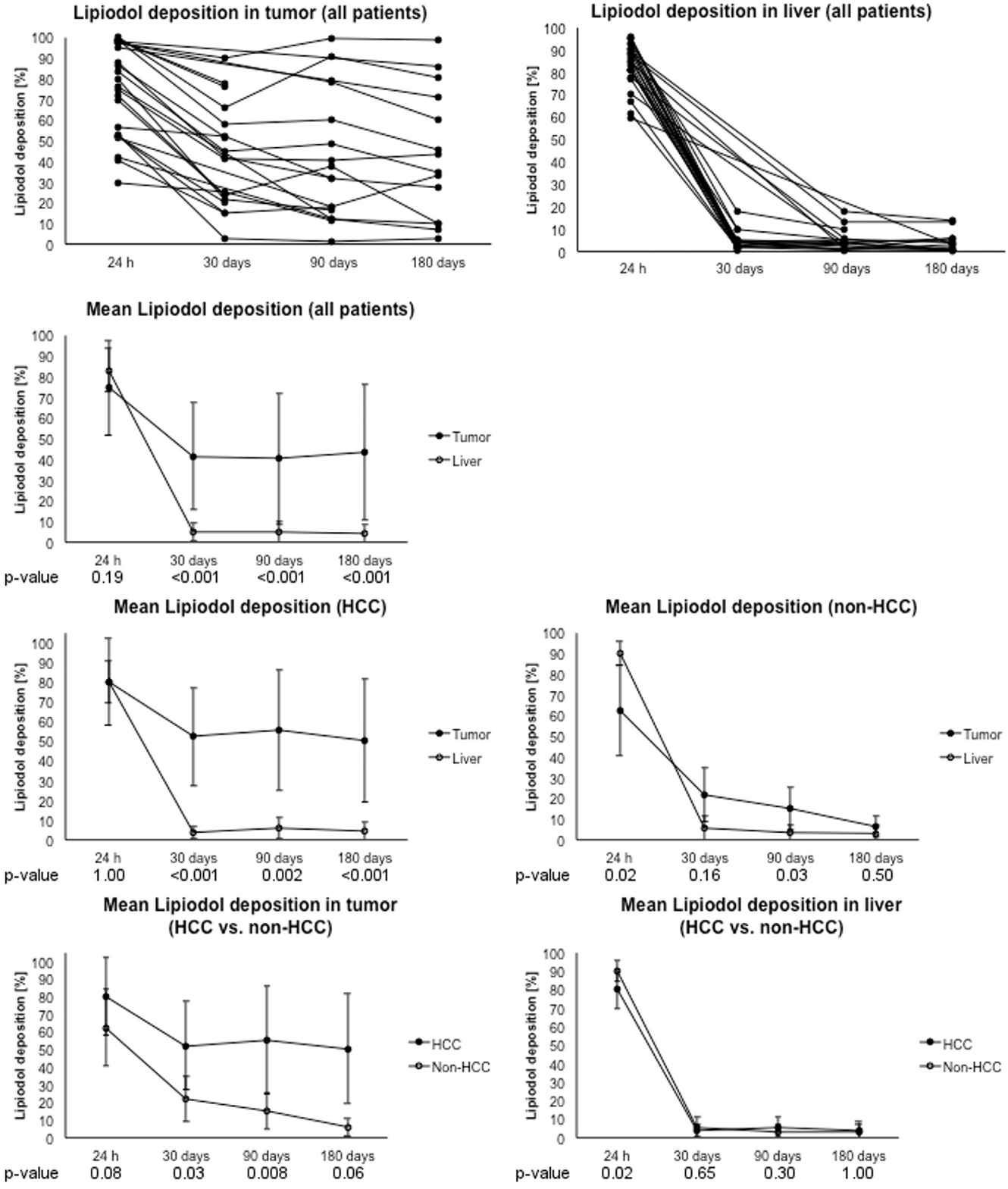

Figure 3. A comparison of the Lipiodol deposition in tumor and in liver tissue, presented for all patients as well as stratified by tumor type (HCC vs. non-HCC).

A key finding of our study linked the extent of baseline tumor enhancement and percentage tumor coverage with Lipiodol on immediate postprocedural CT with higher tumor response rates on follow-up imaging. This trend was more apparent in HCC. Several retrospective studies have reported on the relationship between Lipiodol deposition and longer survival [19,28–33], and some authors reported an association between complete Lipiodol tumor coverage with a lower local tumor recurrence rate [34]. The imaging follow-up period in our study was relatively short, and the trial design did not include time-to-tumor progression as an endpoint. However, no tumor recurrence was observed in tumors with high Lipiodol deposition and complete response by imaging. Taken together, our data prospectively support existing reports acquired retrospectively that correlated Lipiodol deposition with high rates of tumor response [35] and tumor necrosis at histopathology [30,35,36].

Regarding the assessment of tumor response, all enhancement-based techniques detected responders early, indicating a decreased tumor enhancement. However, size-based criteria failed to reliably detect tumor response 30 days after cTACE and had a delayed ability to detect a response. This finding underlines the necessity of using enhancement-based response criteria in the setting of cTACE.

Several factors influence Lipiodol uptake and retention by the targeted tumors. First, Lipiodol is administered intraarterially, which is the preferential blood supply to liver tumors guaranteeing successful targeting of the tumors, while at the same time, dominant portovenous flow to the liver tissue provides a route for the elimination of Lipiodol. Second, it is likely that the various patterns of Lipiodol deposition and retention in tumors reflect inherent tumor characteristics that are not completely clear. It seems however that vascular characteristics of liver tumors may help provide some insight into such patterns of Lipiodol uptake and retention. Finally, it is also possible that the ratio of Lipiodol to chemosolution and the mechanics of emulsion generation may have some impact on the patterns of Lipiodol deposition and retention [15].

The main limitation of this study is the small number of patients, resulting in a lower statistical power. This was countered by a standardized imaging protocol that included a broad range of imaging modalities (MR, CT, and FDG-PET) with different characteristics and properties, allowing a true multiparametric assessment of the tumor and surrounding tissue to be performed. A second limitation of the study was the inclusion of both HCC and non-HCC patients, resulting in a heterogeneous group of patients. However, it was the intended goal of our study to acquire data on a variety of tumor types to enrich the diversity of the role of Lipiodol as a potential reliable imaging biomarker. Finally, no pathological correlation of the radiological findings was obtained.

In summary, our findings confirm the findings from previous animal studies and validate the unique properties and function of Lipiodol as a tumor-specific, drug-carrying, and imaging biomarker agent when used during cTACE to treat patients with primary and secondary liver cancer.

Acknowledgement

Geliang Gan and Yanhong Deng kindly provided statistical advice for this manuscript.

The authors thank Guerbet pharmacueticals for providing funding for this study. The authors of this manuscript declare relationships with the following companies: T.S. Guerbet. J. F. G. received support from Biocompatibles/BTG, Bayer HealthCare, Philips Medical, Nordion/BTG, Guerbet, DOD and NCI-ECOG; M. L. is a Viage Imaging Research North America employee.

This study has also received funding by NIH/NCI (R01 CA160771) and the Rolf W. Günther Foundation for Radiological Science.

Appendix A. Supplementary data

Supplementary data to this article can be found online at https://doi.org/10.1016/j.tranon.2020.01.003.

References

[1] World Health Organization cancer fact-sheet. https://www.who.int/news-room/fact-sheets/detail/cancer (14.08.2019)
[2] J Bruix, JM Llovet, Prognostic prediction and treatment strategy in hepatocellular carcinoma, Hepatology 35 (2002) 519–524.
[3] A Forner, JM Llovet, J Bruix, Hepatocellular carcinoma, Lancet 379 (2012) 1245–1255.
[4] ZV Fong, KK Tanabe, The clinical management of hepatocellular carcinoma in the United States, Europe, and Asia: a comprehensive and evidence-based comparison and review, Cancer 120 (2014) 2824–2838.
[5] R Lencioni, T de Baere, MC Soulen, WS Rilling, JF Geschwind, Lipiodol transarterial chemoembolization for hepatocellular carcinoma: a systematic review of efficacy and safety data, Hepatology 64 (2016) 106–116.
[6] JMM van Breugel, JF Geschwind, S Mirpour, et al., Theranostic application of lipiodol for transarterial chemoembolization in a VX2 rabbit liver tumor model, Theranostics, 2019.
[7] L. European Association, For The Study Of The, R. European Organisation For and C. Treatment Of. EASL-EORTC clinical practice guidelines: management of hepatocellular carcinoma, J Hepatol 56 (2012) 908–943.
[8] J Bruix, M Sherman, D. American Association for the Study of Liver. Management of hepatocellular carcinoma: an update, Hepatology 53 (2011) 1020–1022.
[9] B Gorodetski, J Chapiro, R Schernthaner, et al., Advanced-stage hepatocellular carcinoma with portal vein thrombosis: conventional versus drug-eluting beads transcatheter arterial chemoembolization, Eur Radiol 27 (2) (2017) 526–535.
[10] R Golfieri, E Giampalma, M Renzulli, et al., Randomised controlled trial of doxorubicin-eluting beads vs conventional chemoembolisation for hepatocellular carcinoma, Br J Cancer 111 (2014) 255–264.
[11] RC Martin 2nd, E Bruenderman, A Cohn, et al., Sorafenib use for recurrent hepatocellular cancer after resection or transplantation: observations from a US regional analysis of the GIDEON registry, Am J Surg 213 (4) (2017) 688–695.
[12] JM Llovet, J Bruix, Systematic review of randomized trials for unresectable hepatocellular carcinoma: chemoembolization improves survival, Hepatology 37 (2003) 429–442.
[13] C Camma, F Schepis, A Orlando, et al., Transarterial chemoembolization for unresectable hepatocellular carcinoma: meta-analysis of randomized controlled trials, Radiology 224 (2002) 47–54.
[14] K Memon, RJ Lewandowski, A Riaz, R Salem, Chemoembolization and radioembolization for metastatic disease to the liver: available data and future studies, Curr Treat Options Oncol 13 (2012) 403–415.
[15] JM Idee, B Guiu, Use of Lipiodol as a drug-delivery system for transcatheter arterial chemoembolization of hepatocellular carcinoma: a review, Crit Rev Oncol Hematol 88 (2013) 530–549.
[16] CS Chen, FK Li, CY Guo, et al., Tumor vascularity and lipiodol deposition as early radiological markers for predicting risk of disease progression in patients with unresectable hepatocellular carcinoma after transarterial chemoembolization, Oncotarget 7 (2016) 7241–7252.
[17] SJ Kim, MS Choi, JY Kang, et al., Prediction of complete necrosis of hepatocellular carcinoma treated with transarterial chemoembolization prior to liver transplantation, Gut and liver 3 (2009) 285–291.
[18] DB Hasdemir, LA Davila, N Schweitzer, et al., Evaluation of CT vascularization patterns for survival prognosis in patients with hepatocellular carcinoma treated by conventional TACE, Diagnostic and interventional radiology (Ankara, Turkey) 23 (2017) 217–222.
[19] L Mondazzi, R Bottelli, G Brambilla, et al., Transarterial oily chemoembolization for the treatment of hepatocellular carcinoma: a multivariate analysis of prognostic factors, Hepatology 19 (1994) 1115–1123.
[20] J Chapiro, R Duran, M Lin, et al., Early survival prediction after intra-arterial therapies: a 3D quantitative MRI assessment of tumour response after TACE or radioembolization of colorectal cancer metastases to the liver, Eur Radiol 25 (2015) 1993–2003.
[21] J Chapiro, LD Wood, M Lin, et al., Radiologic-pathologic analysis of contrast-enhanced and diffusion-weighted MR imaging in patients with HCC after TACE: diagnostic accuracy of 3D quantitative image analysis, Radiology 273 (2014) 746–758.
[22] P Therasse, SG Arbuck, EA Eisenhauer, et al., New guidelines to evaluate the response to treatment in solid tumors. European Organization for Research and Treatment of Cancer, National Cancer Institute of the United States, National Cancer Institute of Canada, J Natl Cancer Inst 92 (2000) 205–216.
[23] J Bruix, M Sherman, JM Llovet, et al., Clinical management of hepatocellular carcinoma. Conclusions of the Barcelona-2000 EASL conference. European Association for the Study of the Liver, J Hepatol 35 (2001) 421–430.
[24] R Lencioni, JM Llovet, Modified RECIST (mRECIST) assessment for hepatocellular carcinoma, Semin Liver Dis 30 (2010) 52–60.
[25] AB Miller, B Hoogstraten, M Staquet, A Winkler, Reporting results of cancer treatment, Cancer 47 (1981) 207–214.
[26] J Chapiro, R Duran, M Lin, et al., Identifying staging markers for hepatocellular carcinoma before transarterial chemoembolization: comparison of three-dimensional quantitative versus non-three-dimensional imaging markers, Radiology 275 (2015) 438–447.
[27] FN Fleckenstein, RE Schernthaner, R Duran, et al., 3D Quantitative tumour burden analysis in patients with hepatocellular carcinoma before TACE: comparing single-lesion vs. multi-lesion imaging biomarkers as predictors of patient survival, Eur Radiol 26 (9) (2016) 3243–3252.
[28] DY Kim, HJ Ryu, JY Choi, et al., Radiological response predicts survival following transarterial chemoembolisation in patients with unresectable hepatocellular carcinoma, Aliment Pharmacol Ther 35 (2012) 1343–1350.
[29] HS Lee, KM Kim, JH Yoon, et al., Therapeutic efficacy of transcatheter arterial chemoembolization as compared with hepatic resection in hepatocellular carcinoma patients with compensated liver function in a hepatitis B virus-endemic area: a prospective cohort study, J Clin Oncol 20 (2002) 4459–4465.
[30] WL Monsky, I Kim, S Loh, et al., Semiautomated segmentation for volumetric analysis of intratumoral ethiodol uptake and subsequent tumor necrosis after chemoembolization, AJR Am J Roentgenol 195 (2010) 1220–1230.
[31] SC Yu, JW Hui, EP Hui, et al., Embolization efficacy and treatment effectiveness of transarterial therapy for unresectable hepatocellular carcinoma: a case-controlled comparison of transarterial ethanol ablation with lipiodol-ethanol mixture versus transcatheter arterial chemoembolization, Journal of vascular and interventional radiology : JVIR 20 (2009) 352–359.
[32] TJ Vogl, M Trapp, H Schroeder, et al., Transarterial chemoembolization for hepatocellular carcinoma: volumetric and morphologic CT criteria for assessment of prognosis and therapeutic success-results from a liver transplantation center, Radiology 214 (2000) 349–357.
[33] J Dumortier, F Chapuis, O Borson, et al., Unresectable hepatocellular carcinoma: survival and prognostic factors after lipiodol chemoembolisation in 89 patients, Dig Liver Dis 38 (2006) 125–133.

[34] K Takayasu, Y Muramatsu, T Maeda, et al., Targeted transarterial oily chemoembolization for small foci of hepatocellular carcinoma using a unified helical CT and angiography system: analysis of factors affecting local recurrence and survival rates, AJR Am J Roentgenol 176 (2001) 681–688.

[35] Z Wang, R Chen, R Duran, et al., Intraprocedural 3D quantification of lipiodol deposition on cone-beam CT predicts tumor response after transarterial chemoembolization in patients with hepatocellular carcinoma, Cardiovasc Intervent Radiol 38 (2015) 1548–1556.

[36] S Herber, S Biesterfeld, U Franz, et al., Correlation of multislice CT and histomorphology in HCC following TACE: predictors of outcome, Cardiovasc Intervent Radiol 31 (2008) 768–777.

[38] T Fujita, K Ito, M Tanabe, S Yamatogi, H Sasai, N Matsunaga, Iodized oil accumulation in hypervascular hepatocellular carcinoma after transcatheter arterial chemoembolization: comparison of imaging findings with CT during hepatic arteriography, Journal of vascular and interventional radiology : JVIR 19 (2008) 333–341.

[39] JC Sisson, B Shapiro, WH Beierwaltes, et al., Radiopharmaceutical treatment of malignant pheochromocytoma, J Nucl Med 25 (1984) 197–206.

[40] DY Lee, KC Li, Molecular theranostics: a primer for the imaging professional, AJR Am J Roentgenol 197 (2011) 318–324.